

## PROPAGATING THE FLUID MODEL OF PRODUCTION PROCESSES WITH TIME DELAY

KENJI SHIRAI<sup>1</sup> AND YOSHINORI AMANO<sup>2</sup>

<sup>1</sup>Faculty of Information Culture  
Niigata University of International and Information Studies  
3-1-1, Mizukino, Nishi-ku, Niigata 950-2292, Japan  
shirai@nuis.ac.jp

<sup>2</sup>Kyohnan Elecs Co., LTD.  
8-48-2, Fukakusanishiura-cho, Fushimi-ku, Kyoto 612-0029, Japan  
y\_amano@kyohnan-elecs.co.jp

Received April 2018; revised August 2018

**ABSTRACT.** *Process delay may largely reduce the production revenues of a business, particularly in small- and medium-sized enterprises. In our previous report, the production process was treated as a propagating fluid, and its delay was assumed as a lead time delay. As a new perspective, the downstream process is delayed by restraining the propagation of the upstream process. Moreover, we present that the propagation model with delay is equivalent to an Ornstein-Uhlenbeck (OU) process in mathematical finance. To obtain the parameters of the delay time and process stages, the stationary transition distribution is solved by analyzing the Fokker-Plank equation in numerical simulations. The types of production flow systems corresponding to different transition distributions are also analyzed.*

**Keywords:** Lead time delay, Throughput, Langevin equation, Ornstein-Uhlenbeck process, Production process

**1. Introduction.** In small- and medium-sized enterprises, human intervention constitutes a significant part of the production process, and revenue can sometimes be greatly affected by human behavior. Therefore, with respect to human intervention with outside companies, a deep analysis of the production process and human collaboration is necessary to understand the potential negative effects of human intervention [1, 2]. Naturally, the effect of human behavior is not just a problem with small- and medium-sized companies; it must be regarded as one of the major problems that may occur when humans directly intervene in the production process [3, 4, 5].

In general, the potential uncertainties should be considered before proceeding with a system that combines human intervention (internal force) with outside companies (external force) in the production system [6, 7]. With respect to two elements in a production system, a total system is formed by connecting the two elements. In this case, a system with certain uncertainties will be formed when connecting “human intervention” and “outside companies” in a production system. In general, an important concept in the production system is to develop the best system that results in efficient production. However, in most analysis of the production process, researchers have not taken advantage of the noise inherent in the system. Such noise may have unique usefulness in the system.

The improvement of productivity and the evaluation method in the manufacturing industry have been discussed for many years [8, 9]. In the manufacturing industry, TOC

(Theory of Constraints) was synonymous with basic productivity improvement. This is an Israeli physicist, Dr. Eriq Gold Rat who has pioneered about 25 years ago. It is a methodology of system improvement [10]. Small fluctuations in an upstream subsystem appear as large fluctuations in the downstream (the so-called bullwhip effect) [4]. The bullwhip effect generates a large gap between the demand forecasts of the market and suppliers. Large fluctuations can be suppressed by the following mechanisms.

- Reducing the lead time, improving the throughput, and synchronizing the production process by the TOC.
- Sharing the demand information and performing mathematical evaluations.
- Analyzing the reduction and fluctuating demands of the subsystem (using nonlinear vibration theory).
- Basing the inventory management approach on stochastic demand.

We have been studying a mathematical modeling and improvement of production processes over the years. We have reported that a simple exclusion process is a non-equilibrium statistical mechanics model called a one-dimensional asymmetric simple exclusion process (ASEP) [11]. The ASEP is used in production lines to improve production efficiency. As an application method, the ASEP is used to optimize the production lot [12].

We have used the ASEP to improve the efficiency of the production process. When applied as a model of a lot production system, the ASEP is fundamentally a nonlinear system represented by Burgers' equation. This indicates that the process transition probability plays an important role. From the experience of three test runs of the production flow process (PFP), we have evaluated the ASEP as being effective for improving production efficiency because of the number of lots in the production line. As a result, twice the throughput was obtained compared to the conventional PFP method, and the production cost was reduced by 20% [11]. Then, one profit-controlling factor in the manufacturing business is inventory-asset management. We have reported the method that manages inventory assets at the end of the fiscal year, that is, the method is based on the route-dependent options of mathematical finance and is validated in a theoretical verification based on inventory assets over five years (from 2007 to 2011). Suitable inventory asset management is essential to keep a profit.

There seem to be few reports using mathematical finance regarding inventory management [13]. Regarding bottleneck analysis in the production process, we have analyzed mathematically the phenomena that occur before and after an interruption to production processes. We have also analyzed the resulting shock wave propagation of production density flows using Burgers' equation [14]. To enable efficient application to a production system, by performing the synchronization process, the throughput for the manufacturing process is reduced [2]. We have utilized Burgers' equation for analyzing the fluctuations in the lead time of production processes [14, 15]. The factors causing fluctuations include the following:

- Uncertainty of logistics
- Uncertainty of production planning
- Stochastic characteristics of the order and start time series

We clarified that the fluctuations in lead time were dependent on the state variable, which was a throughput deviation. The propagation of throughput deviation was restricted by Burgers' equation of fluid dynamics. In our previous study, we reported that the normalized lead time data had an on-off intermittency [16]. To verify our analysis, we represented actual data that were obtained before/after the managing of processes using the cyclic production flow process [3]. Then, we have clarified the relation between

lead time and production density by constructing two stochastic differential equations as a mathematical model. We have also clarified that production density is greatly affected by a fluctuation in lead time [17]. Moreover, we have reported an analysis of production processes using a lead-time function. Two types of production demand are classified in a production business. One is custom-type production (asynchronous type), which has a stochastic element. The other is mass-produced production (synchronous type), which has almost no stochastic element. We have reported an optimal production allocation to maximize the rate of increase in cash flow by these two types of production requests (complex type). Our approach is to take advantage of the risk-sensitive control method, which is a powerful technique that takes robustness into account [18].

This study assumes product lead time as process delay. The reason is to make the mathematical modeling of production process easier to understand. Further, this study assumes that the specified control equipment is ordered by a customer and is classified into a number of production elements during the production process. The finished product is then delivered to the customer. Any process delay may largely impact the business production revenues, particularly those of small- and medium-sized enterprises. A company must determine a proper lead time during which the production can continue in a state of incomplete information. However, the inherent noise in the production system, which may play a unique and beneficial role, has rarely been exploited in production process analyses.

As a new perspective, the process delay limits the downstream process by restraining the propagation in the upstream process. The propagation model with delay is equivalent to an Ornstein-Uhlenbeck (OU) process in mathematical finance. Finally, the parameters of the delay time and process stages are reported in numerical simulations of the stationary transition distribution, obtained by analyzing the Fokker-Plank equation [19, 20]. A type of production flow system (typified by Test-runs 1, 2, 3, or 4) is assigned to the transition distribution. To the best of our knowledge, productive processes have not been previously analyzed from this perspective.

**2. Production Systems in the Manufacturing Equipment Industry.** In Figure 1, we briefly represent the manufacturing method used in manufacturing equipment. More information is provided in our report [21]. This system is regarded as “Make-to-order system with version control”, which enables manufacturing after receipt of orders from customers, resulting in “volatility” according to its delivery date and lead time. In addition, there is volatility in lead time depending on the content of the make-to-order products (production equipment).

The company in this study is the “supplier” in Figure 1 and “factory” here. Companies are under the assumption that there are  $N$  (numbers of) suppliers; however, this study deals with one company because no data is published for the rest of the companies ( $N - 1$ ).

**2.1. Production flow process.** A manufacturing process that is termed as a production flow process is shown in Figure 2. The production flow process, which manufactures low volumes of a wide variety of products, is produced through several stages in the production process. In Figure 2, the processes consist of six stages. In each step S1-S6 of the manufacturing process, materials are being produced. The direction of the arrows represents the direction of the production flow. Production materials are supplied through the inlet and the end-product is shipped from the outlet [3].

**2.2. Propagation of production density.** Figure 3 shows that connections between processes can be treated as diffusive propagation of product [1]. In Figure 3,  $u$  and  $n$  represent the throughput and production density, respectively [1]. In fluid dynamics,

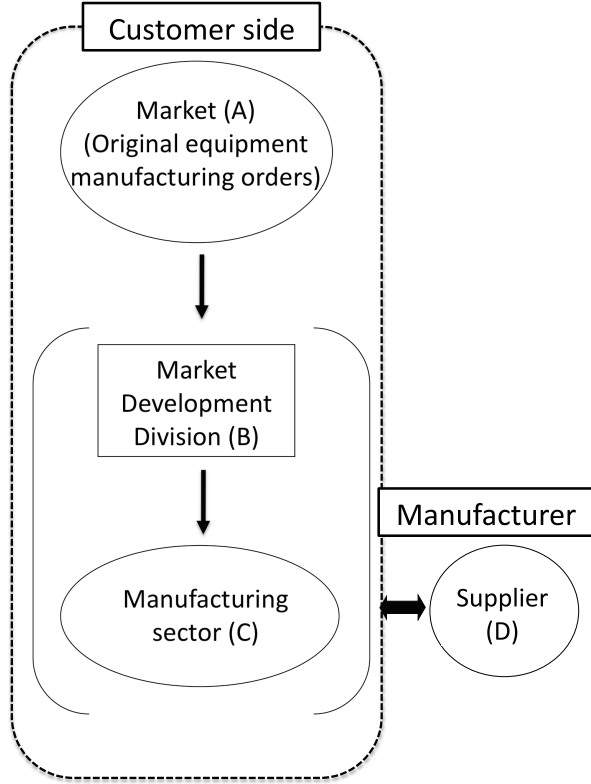


FIGURE 1. Business association chart of company of research target

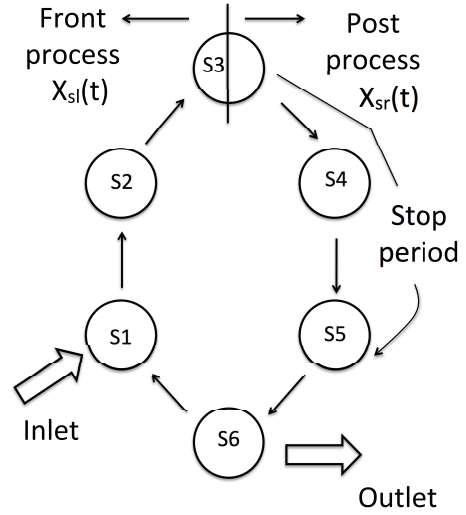


FIGURE 2. Bottleneck period in production flow processes

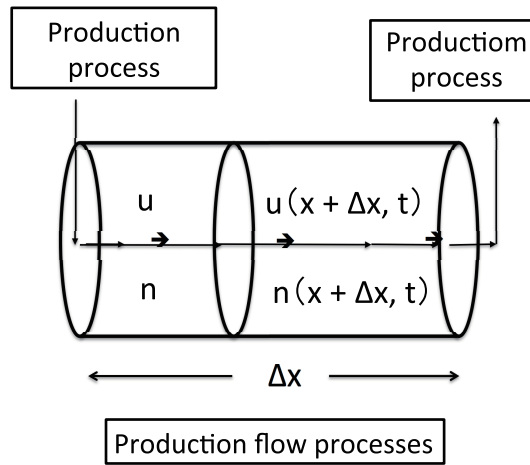


FIGURE 3. Propagation flow

$S$  represents the cross-sectional area and the numerical density continuous equation is written as follows [15].

$$\Delta(nS\Delta x) = n(t, x)u(t, x)\Delta tS - n(t, x + \Delta x)u(t, x + \Delta x)\Delta t \tag{1}$$

$$\left(\frac{\Delta n}{\Delta t}\right)_x = -\frac{n(t, x + \Delta x)u(t, x + \Delta x) - n(t, x)u(t, x)}{\Delta x} \tag{2}$$

$$\frac{\partial n}{\partial t} = -\frac{\partial(nu)}{\partial x} \tag{3}$$

In the left-hand side the second term  $u \frac{\partial u}{\partial t}$  is the advection term. Now, let  $u = c$  (constant value), we consider the following equation.

$$\frac{\partial}{\partial t}u + c \frac{\partial}{\partial x}u = 0 \quad (4)$$

Equation (4) represents a linear wave motion traveling to  $+x$  direction at a constant speed  $c$ . Figure 2 shows the production process. This production process is used for manufacturing a control device. The bottleneck occurs at some stage in the process of Figure 2.

### 3. Delay Model by Langevin Equation.

**3.1. Ornstein-Uhlenbeck (OU) process.** OU process is a stochastic process  $r_t$  given by the following stochastic differential equations.

$$dr_t = -\theta(r_t - \mu)dt + \sigma dW_t \quad (5)$$

where  $\theta$ ,  $\mu$  and  $\sigma$  are parameters.  $W_t$  is a Wiener process.

Equation (5) is the Langevin equation physically and can be solved by a variation of constants [20].

**Definition 3.1.**

$$f(r_t, t) = r_t \exp(\theta t) \quad (6)$$

By applying Ito's lemma to the left hand side of Equation (6) we obtain the following equation.

$$f(r_t, t) = \exp(\theta t)\theta\mu dt + \sigma \exp(\theta t)dr_t \quad (7)$$

Integrating Equation (7) from 0 to  $t$ , we obtain the following equation.

$$r_t = r_0 \exp(-\theta t) + \mu(1 - \exp(-\theta t)) + \int_0^t \sigma \exp(\theta(s - t))dW_s \quad (8)$$

where  $r_0$  is an initial value (constant).

### 3.2. Fokker Planck's equation and its stationary solution.

**Definition 3.2.**  $h^0(t)$  is a spatial uniform function in  $h(t)$ .

When the steady distribution of the transition probability satisfies  $h(t) \leq k$ , the range of maximum values of the transition probability narrows as  $\beta \rightarrow 1$ .

$$\beta = \frac{m}{a}, \quad |m| \leq 0.5 \quad (9)$$

As  $\beta$  increases,  $a$  approaches zero; that is, the deviation width becomes small.

Now, let the time lag with waiting constraint  $d$  be expressed by Langevin equation as follows [20].

$$\frac{dh}{dt} = -\beta h(t - d) + \xi(t), \quad \langle \xi(t) \cdot \xi(t') \rangle = \delta(t - t') \quad (10)$$

where  $\beta$  and  $\xi(t)$  are the drift coefficient and an external force, respectively.

According to Vasicek model [7], the stochastic delay can be modeled as the following Langevin equation under a potential field:

$$\frac{dh(t)}{dt} = a\{W_{opt}(\Delta\varphi) - h(t)\} + \sqrt{H}r(t) \quad (11)$$

where  $\Delta\varphi = h(t) - h^0$ .  $h^0$  denotes an equilibrium point (synchronous point) and  $W_{opt}(\Delta\varphi)$  denotes an optimal throughput function, which was calculated according to  $\Delta\varphi$ , and is a  $C^\infty$  function.  $\sqrt{H}r(t)$  is a noise term [22].

We considered that it corresponds to the Wiener term by considering noise terms as stochastic differential equation. Therefore, Equation (11) is described as a Wiener model, which is an Ornstein-Uhlenbeck (OU) process, as follows.

$$dh(t) = -a(h(t) - \mu) + \sigma dW_t \quad (12)$$

where  $a$ ,  $\mu$ ,  $\sigma$  and  $dW_t$  are a constant parameter, trend parameter, volatility and Wiener process respectively.

We obtain the second order Fokker-Plank equation in  $x$  and the first order in  $t$  and  $d$  using the expansion of step operator as follows.

$$\frac{\partial}{\partial d} P_e(z, s, d) = \frac{\partial}{\partial x} [(\beta s) P_e(z, s, d)] + \frac{1}{2} \frac{\partial^2}{\partial z^2} P_e(z, s, d) \quad (13)$$

where the boundary condition is derived as follows.

$$P_e(z, s, d = 0) = \sqrt{\frac{\beta}{\pi}} e^{-\beta x^2} \delta(z - s) \quad (14)$$

The stationary solution of Equation (13) should be identical for the OU process as follows [20].

$$P_e(z, s, d) = \left( \sqrt{\frac{\beta}{\pi}} \exp\left\{-\frac{1}{2}\beta^2 s^2 d - \beta z s\right\} \right) \times \left\{ \frac{1}{\sqrt{2\pi d}} \exp\left(-\frac{(z - s)^2}{2d}\right) \right\} \quad (15)$$

Refer to Appendix A for derivation of Equation (15).

## 4. Numerical Simulation.

**4.1. Analysis of the stationary transition probability  $P_e(z, s, d)$ .** The transition probability  $P_e(z, s, d)$  is proportional to the drift coefficient  $\beta$ , as described below.

- $P_e(z, s, d)$  depends on both the initial stage with no delay  $\delta(z - s)$  and the drift coefficient  $\beta$ .
- $P_e(z, s, d)$  depicts the normal distribution with volatility, which is proportional to the delay  $d$ , at each stage. The delay parameter  $d$  within each stage width is zero.

The transition probability  $P_e(z, s, d)$  is a function of  $s$ , with  $|s| \leq a$ . Its properties are as follows.

- When  $\beta \ll 0$ ,  $P_e(z, s, d)$  is affected by delay  $d$ , but there is also a tendency for strong coupling to  $s$  to a relatively wide range of  $z$ .
- When  $\beta \gg 0$ , as the delay  $d$  increases,  $s$  approaches zero. In this case, there is a tendency that the coupling with the nearest stage becomes stronger.

Figure 4 shows that the delay  $d = 1$  and the drift coefficient  $\beta = 0.15$ . Table 1 represents the graphs for the value of  $s$  in Figure 4. When  $s = 0$ , the coupling with the nearest stage becomes stronger. As  $s$  increases, the coupling of stage becomes stronger for a wide range of stages.

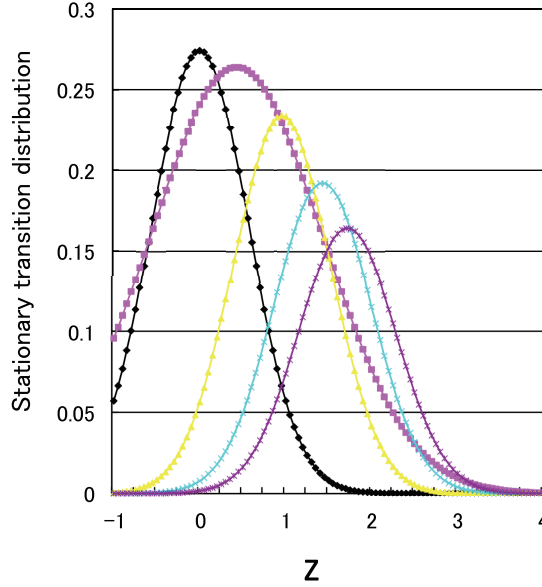


FIGURE 4. (color online) Langevin model with delay ( $\beta = 0.15$ , Delay = 1)

TABLE 1. Stationary transition probability distribution

	“Black”	“Pink”	“Yellow”	“Blue”	“Purple”
$s$	0	0.5	1.0	1.5	1.8

4.2. **Analysis of Test-runs 1-4.** In Test-run 1 (asynchronous method), the lead time was set to “WS (working standard)”, as shown in Table 4 of Appendix B. When the lead time is small, the WS imposes a strong connection between the stages (S1 to S6). The lead time correlates with the total drift (equal throughput = 0.73). In Test-run 2 (synchronous method), where the lead time is large, WS in Table 6 imposes a weak coupling between the stages (S1 to S6). This lead time also correlates with the total drift (equal throughput = 0.92). The total drift values depict the total working time of nine workers (K1-K9) at each stage (S1-S6) (see Tables 4, 6 and 10 in Appendix B).

The area designated “A” in Figure 5 appears over a wide range of lead time deviations (indicating low throughput and high volatility). In contrast, area “B” occurs over a narrow range of lead time deviations (indicating high throughput and low volatility).

- “A”:  $\beta$  is a constant and  $d$  is large.  $\beta$  is large and  $d$  is a constant.
- “B”:  $\beta$  is a constant and  $d$  is small.  $\beta$  is small and  $d$  is a constant.

To maintain high-throughput production (within area “B” in Figure 5), the workers must be appropriately organized to reduce the volatility over the whole production process. The optimal selection will maintain  $\beta$  and  $d$  in area “B” of Figure 5.

We have already evaluated and reported the production throughput in a mathematical finance analysis. Assuming that the production throughput behaves as an OU process, we theoretically analyzed the asynchronous and synchronous processes in the production. Three patterns, which combined the asynchronous and synchronous methods of each of the nine workers throughout the six stages, were also tested. Synchronous methods were identified as more effective than asynchronous method [3].

Next, we determined the number of deviations between the set lead time (WS) and the working time of the nine workers at each stage. The results are presented in Table 2. Here, the WS and drift are correlated in the actual data of a production flow process.

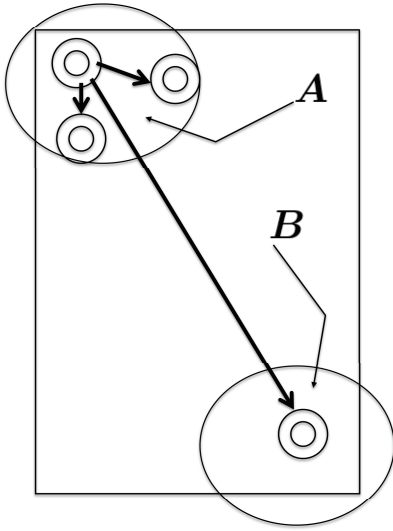


FIGURE 5. Variation of the stationary transition probability  $P_e(z, s, d)$  by  $d$  and  $\beta$

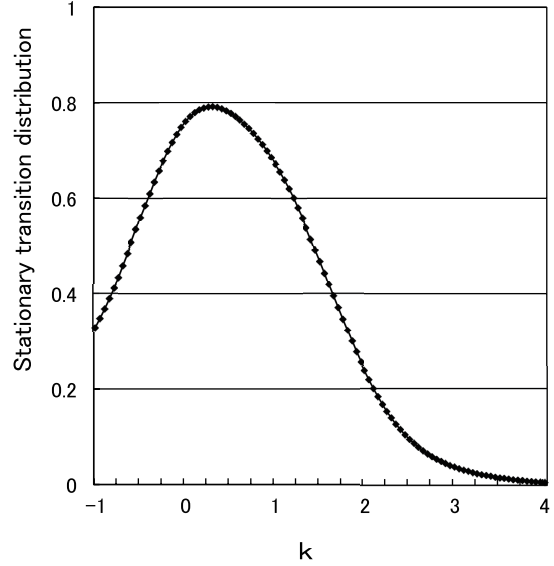


FIGURE 6. Joint stationary transition probability with delay ( $\beta = 0.5$ , Delay = 0.5)

TABLE 2. Stationary transition probability distribution

Evaluation standard	Test-run 1	Test-run 2	Test-run 3	Test-run 4
$\delta K < 5$	6	7	8	26
$\delta K < 4$	6	3	5	23
$\delta K < 3$	5	0	5	20
$\delta K < 2$	4	0	5	20
$\delta K < 1$	2	0	3	8
Drift value	0.73	0.92	0.95	0.95
Volatility	0.29	0.06	0.03	0.03

Figure 6 depicts a joint stationary transition distribution with  $\beta = 0.5$  and delay  $d = 0.5$ . As shown in Figures 6-8, increasing the  $d$  shifts the distribution to the left and raises its peak value. The joint stationary transition probability with delay shows the same characteristics as the stationary transition probability with delay.

The relations between the stationary transition probability and working time in Test-runs 1-4 exhibit the following behaviors.

- Retaining  $\beta$  constant and increasing  $d$  distributes the stationary transition probability over a wide range of the process stages ( $s$ ), which delays the lead time of each stage. This phenomenon, which corresponds to Test-run 1, appears because the result exceeds the WS value in almost all stages (indicated by the encircled values in Table 4).
- When  $d$  is small, the stationary transition probability distribution is narrow and the process delay is limited. In a limited number of cases, the distribution deviates from the reference value (encircled values in Tables 6 and 10). In particular, when  $d$  is small, the stationary transition probability distribution approaches zero as the process proceeds, which means that the influence of the delay vanishes. This situation well corresponds with Test-runs 2-4. In Test-run 4, some data are below

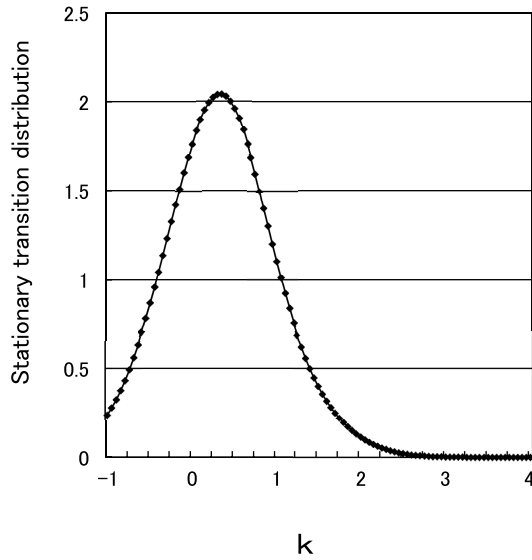


FIGURE 7. Joint stationary transition probability with delay ( $\beta = 0.5$ , Delay = 5)

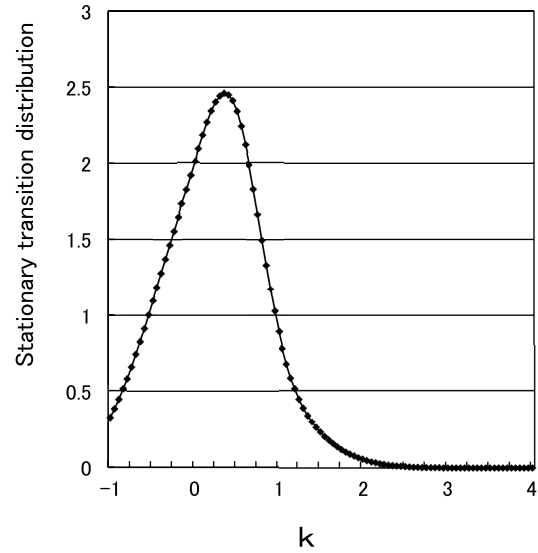


FIGURE 8. Joint stationary transition probability with delay ( $\beta = 0.5$ , Delay = 10)

the WS (encircled values in Table 10), implying that Test-run 4 has the shortest throughput.

**5. Conclusion.** As a summary in our report, regarding the process delay as a lead time delay, we have reported that the process delay limits the downstream process by restraining the propagation in the upstream process. Subsequently, we mathematically modeled the processing delay as an OU process. When the delay is large, a stationary transition distribution (corresponding to Test-run 1) appears in all in-process stages. We also verified that when the delay is small, a limited steady-state transition distribution (corresponding to Test-runs 2-4) appears in the in-process stage.

The future study will involve the application of the potential theory to quality thresholds and quality fluctuations.

**REFERENCES**

- [1] K. Shirai and Y. Amano, Prduction density diffusion equation and production, *IEEJ Trans. Electronics, Information and Systems*, vol.132-C, no.6, pp.983-990, 2012.
- [2] K. Shirai and Y. Amano, A study on mathematical analysis of manufacturing lead time -Application for deadline scheduling in manufacturing system-, *IEEJ Trans. Electronics, Information and Systems*, vol.132-C, no.12, pp.1973-1981, 2012.
- [3] K. Shirai, Y. Amano and S. Omatu, Improving throughput by considering the production process, *International Journal of Innovative Computing, Information and Control*, vol.9, no.12, pp.4917-4930, 2013.
- [4] K. Shirai, Y. Amano and S. Omatu, Propagation of working-time delay in production, *International Journal of Innovative Computing, Information and Control*, vol.10, no.1, pp.169-182, 2014.
- [5] K. Shirai and Y. Amano, Throughput improvement strategy for nonlinear characteristics in the production processes, *International Journal of Innovative Computing, Information and Control*, vol.10, no.6, pp.1983-1997, 2014.
- [6] K. Shirai, Y. Amano and S. Omatu, Process throughput analysis for manufacturing process under incomplete information based on physical approach, *International Journal of Innovative Computing, Information and Control*, vol.9, no.11, pp.4431-4445, 2013.
- [7] K. Shirai and Y. Amano, Production throughput evaluation using the Vasicek model, *International Journal of Innovative Computing, Information and Control*, vol.11, no.1, pp.1-17, 2015.
- [8] M. E. Mundel, *Improving Productivity and Effectness*, Prentice-Hall, NZ, 1983.

- [9] A. Neely, M. Gregory and K. Platts, Performance measurement system design, *International Journal of Operations & Production Management*, vol.15, no.4, pp.5-16, 1995.
- [10] S. J. Baderstone and V. J. Mabin, A review Goldratt's Theory of Constraints (TOC) – Lessons from the international literature, *Operations Research Society of New Zealand 33rd Annual Conference*, University of Auckland, New Zealand, 1998.
- [11] K. Shirai and Y. Amano, Production model using an asymmetric simple exclusion process, *International Journal of Innovative Computing, Information and Control*, vol.14, no.1, pp.65-81, 2018.
- [12] N. Nishihira, A control approach of the bullwhip effect in the supply chain: An analysis of time-delay systems via memoryless feedback control, *Yamagata University Humanities Research Annual Report*, vol.5, pp.205-214, 2008.
- [13] K. Shirai and Y. Amano, Suitable inventory asset management using route-dependent options in mathematical finance, *International Journal of Innovative Computing, Information and Control*, vol.13, no.6, pp.1791-1811, 2017.
- [14] K. Shirai and Y. Amano, Production process retention using a flow analysis in the manufacturing business, *International Journal of Innovative Computing, Information and Control*, vol.13, no.5, pp.1491-1507, 2017.
- [15] K. Shirai and Y. Amano, Analysis of fluctuations in production processes using Burgers equation, *International Journal of Innovative Computing, Information and Control*, vol.12, no.5, pp.1615-1628, 2016.
- [16] K. Shirai and Y. Amano, On-off intermittency management for production process improvement, *International Journal of Innovative Computing, Information and Control*, vol.11, no.3, pp.815-831, 2015.
- [17] K. Shirai and Y. Amano, Investigation of the relation between production density and lead-time via stochastic analysis, *International Journal of Innovative Computing, Information and Control*, vol.13, no.4, pp.1117-1133, 2017.
- [18] K. Shirai and Y. Amano, Determination of allocation rate of production projects utilizing risk-sensitive control theory, *International Journal of Innovative Computing, Information and Control*, vol.13, no.3, pp.847-871, 2017.
- [19] D. T. Gillespie, Exact numerical simulation of the Ornstein-Uhlenbeck process and its integral, *Physical Review E*, vol.54, pp.2084-2091, 1996.
- [20] T. Ohira, A Fokker-Planck equation with delay, *Physical Properties Study*, vol.70, no.3, pp.448-451, 1998.
- [21] K. Shirai, Y. Amano, S. Omatu and E. Chikayama, Power-law distribution of rate-of-return deviation and evaluation of cash flow in a control equipment manufacturing company, *International Journal of Innovative Computing, Information and Control*, vol.9, no.3, pp.1095-1112, 2013.
- [22] K. Shirai and Y. Amano, Synchronization analysis of the production process utilizing the phase-field model, *International Journal of Innovative Computing, Information and Control*, vol.12, no.5, pp.1597-1613, 2016.
- [23] K. Shirai and Y. Amano, Evaluation of production process using multimode vibration theory, *International Journal of Innovative Computing, Information and Control*, vol.10, no.3, pp.1161-1178, 2014.
- [24] M. Aida and K. Horikawa, Stability analysis for global performance of flow control in high-speed networks based on statistical physics, *IEICE Trans. Commun.*, vol.E82-B, no.12, 1999.

## Appendix A. Stationary Solution of the Fokker-Plank Equation.

$$P_o(x, s, 0) = \sqrt{\frac{\beta}{\pi}} \exp(-\beta x^2) \delta(x - s) \quad (16)$$

$$P_e(x, s, d) = \frac{1}{\sqrt{2\pi}} \int_{-\infty}^{\infty} P_e(k, s, d) e^{-ikx} dk \quad (17)$$

We obtain as follows after the Fourier transform is executed on Equation (17).

$$\begin{aligned} & \int_{-\infty}^{\infty} \frac{\partial}{\partial d} \left\{ \frac{1}{\sqrt{2\pi}} P_e(k, s, d) e^{-ikx} \right\} dk \\ &= (\beta s) \int_{-\infty}^{\infty} \frac{\partial}{\partial x} \left\{ \frac{1}{\sqrt{2\pi}} P_e(k, s, d) e^{-ikx} \right\} dk + \int_{-\infty}^{\infty} \frac{\partial^2}{\partial x^2} \left\{ \frac{1}{\sqrt{2\pi}} P_e(k, s, d) e^{-ikx} \right\} dk \quad (18) \end{aligned}$$

We obtain as follows after the partial integral of the first term on the right side of Equation (18).

The first term

$$= (\beta s) \int_{-\infty}^{\infty} \left\{ \frac{1}{\sqrt{2\pi}} (ik) P_e(k, s, d) e^{-ikx} \right\} dk - \frac{1}{2} \int_{-\infty}^{\infty} \left\{ \frac{1}{\sqrt{2\pi}} k^2 P_e(k, s, d) e^{-ikx} \right\} dk \quad (19)$$

From Equation (19), we obtain as follows.

$$\begin{aligned} & \int_{-\infty}^{\infty} \left\{ \frac{1}{\sqrt{2\pi}} \left[ \frac{d\tilde{P}_e}{dd} \right] e^{ikx} \right\} dk \\ &= \int_{-\infty}^{\infty} \left\{ \frac{1}{\sqrt{2\pi}} [(\beta isk) \tilde{P}_e] e^{ikx} \right\} dk - \int_{-\infty}^{\infty} \left\{ \frac{1}{\sqrt{2\pi}} \left[ \frac{1}{2} k^2 \tilde{P}_e \right] e^{ikx} \right\} dk \end{aligned} \quad (20)$$

where  $\tilde{P}_e$  defines the function of one variable  $k$  with parameters  $s$  and  $d$ . Therefore, we obtain from the identity condition as follows.

$$\frac{d\tilde{P}_e}{dd} - (\beta isk) \tilde{P}_e + \frac{1}{2} k^2 \tilde{P}_e = 0 \quad (21)$$

The solution of Equation (21) is obtained as follows.

$$\tilde{P}_e = A(k) \exp \left\{ -\frac{1}{2} k^2 - (\beta isk) \right\} t \quad (22)$$

Thus,  $P_e(k, s, d)$  is derived as follows.

$$P_e(k, s, d) = \int_{-\infty}^{\infty} A(k) \exp \left\{ -\frac{1}{2} k^2 - (\beta isk) \right\} t \quad (23)$$

From initial condition  $P_e(x, 0, 0)$ ,  $A(k)$  is derived as follows.

$$P_e(x, 0, 0) = P_{e,0}(x) = \frac{1}{\sqrt{2\pi}} \int_{-\infty}^{\infty} A(k) \exp(-kx) dk \quad (24)$$

$$A(k) = \frac{1}{\sqrt{2\pi}} \int_{-\infty}^{\infty} P_{e,0}(x) \exp(-kx) dx \quad (25)$$

We obtain as follows after multiplying  $\exp(-ikx)$  to Equation (25).

$$\begin{aligned} A(k) \exp(-ikx) &= \frac{1}{\sqrt{2\pi}} \int_{-\infty}^{\infty} P_{e,0}(x) \exp(-kx) \cdot \exp(ikx) dx \\ &= \frac{1}{\sqrt{2\pi}} \int_{-\infty}^{\infty} P_{e,0}(x) \exp\{-(1+i)kx\} dx \end{aligned} \quad (26)$$

We obtain by using Equation (26) to Equation (23) as follows.

$$\begin{aligned} P_e(k, s, d) &= \frac{1}{\sqrt{2\pi}} \int_{-\infty}^{\infty} dk \int_{-\infty}^{\infty} dx' P_{e,0}(x') \exp\{ik(x-x')\} \\ &\quad \times \exp \left\{ -\left( \frac{1}{2} k^2 - (\beta isk) \right) \right\} t \\ &= \int_{-\infty}^{\infty} \exp \left[ \frac{1}{2} k - i \left\{ (\beta s) - \frac{i(x-x')}{2\pi t} \right\} \right]^2 dk \\ &= \sqrt{\frac{\pi}{t}} \left[ \exp \left( -\frac{1}{2} \beta - \beta s x \right) \right] \end{aligned} \quad (27)$$

From Delta theory, we obtain as follows.

$$\int_{-\infty}^{\infty} \sqrt{\frac{\beta}{\pi}} dx' \exp\{-\beta(x-x')^2\} \delta(x-x') = \sqrt{\frac{\beta}{\pi}} \exp(-\beta x) \quad (28)$$

From Equation (28), Equation (23) is obtained as follows.

$$P_e(k, s, d) = \sqrt{\frac{\beta}{\pi}} \exp\left\{-\frac{1}{2}(\beta s)^2 - \beta s x\right\} \left[ \frac{1}{2\sqrt{\pi k t}} \int_{-\infty}^{\infty} dx' \exp\left\{-\frac{(x-x')^2}{4kt}\right\} \right] \quad (29)$$

From Equation (29), we obtain as follows.

$$P_e(k, s, d) = \left[ \sqrt{\frac{\beta}{\pi}} \exp\left\{-\frac{1}{2}(\beta s)^2 d - \beta s x\right\} \right] \left[ \frac{1}{\sqrt{2\pi d}} \exp\left\{-\frac{(x-s)^2}{2d}\right\} \right] \quad (30)$$

### Appendix B. Analysis of the Test-run Results.

- (Test-run 1): Because the throughput of each process (S1-S6) is asynchronous, the overall process throughput is asynchronous. In Table 4, we list the manufacturing time (min) of each process. In Table 5, we list the volatility in each process performed by the workers. Finally, Table 4 lists the target times. The theoretical throughput is obtained as  $3 \times 199 + 2 \times 15 = 627$  (min). In addition, the total working time in stage S3 is 199 (min), which causes a bottleneck. In Figure 9, we plot the measurement data listed in Table 4, which represents the total working time of each worker (K1-K9). In Figure 10, we plot the data contained in Table 4, which represents the volatility of the working times.
- (Test-run 2): Set to synchronously process the throughput. The target time listed in Table 6 is 500 (min), and the theoretical throughput (not including the synchronization idle time) is 400 (min). Table 7 presents the volatility of each working process (S1-S6) for each worker (K1-K9).
- (Test-run 3): Introduce a preprocess stage. The process throughput is performed synchronously with the reclassification of the process. As shown in Table 8, the theoretical throughput (not including the synchronization idle time) is 400 (min). Table 9 presents the volatility of each working process (S1-S6) for each worker (K1-K9).
- (Test-run 4): The same as Test-run 3.  
On the basis of these results, the idle time must be set to 100 (min). Moreover, the theoretical target throughput ( $T'_s$ ) can be obtained using the ‘‘Synchronization with preprocess’’ method. This goal is as follows:

$$\begin{aligned} T_s &\sim 20 \times 6 \text{ (First cycle)} + 17 \times 6 \text{ (Second cycle)} \\ &\quad + 20 \times 6 \text{ (Third cycle)} + 20 \text{ (Previous process)} + 8 \text{ (Idle-time)} \\ &\sim 370 \text{ (min)} \end{aligned} \quad (31)$$

The full synchronous throughput in one stage (20 min) is

$$T'_s = 3 \times 120 + 40 = 400 \text{ (min)} \quad (32)$$

Using the ‘‘Synchronization with preprocess’’ method, the throughput is reduced by approximately 10%. Therefore, we showed that our proposed ‘‘Synchronization with preprocess’’ method is realistic and can be applied in flow production systems. Below, we represent for a description of the ‘‘Synchronization with preprocess’’.

In Table 8, the working times of the workers K4, K7 show shorter than others. However, the working time shows around target time. Next, we manufactured one

piece of equipment in three cycles. To maintain a throughput of six units/day, the production throughput must be as follows:

$$\frac{(60 \times 8 - 28)}{3} \times \frac{1}{6} \simeq 25 \text{ (min)} \tag{33}$$

where the throughput of the preprocess is set to 20 (min). In Equation (33), the value 28 represents the throughput of the preprocess plus the idle time for synchronization. Similarly, the number of processes is 8 and the total number of processes is 9 (8 plus the preprocess). The value of 60 is obtained as 20 (min) × 3 (cycles).

In Table 8 and Table 10, Test-run 3/run 4 indicates a best value for the throughput in the three types of theoretical working time. Test-run 2 is ideal production method. However, because it is difficult for talented worker, Test-run 3/run 4 is a realistic method.

The results are as follows. Here, the trend coefficient, which is the actual number of pieces of equipment/the target number of equipment, represents a factor that indicates the degree of the number of pieces of manufacturing equipment.

- Test-run 1: Drift = 0.29, 4.4 (pieces of equipment)/6 (pieces of equipment) = 0.73
- Test-run 2: Drift = 0.03, 5.5 (pieces of equipment)/6 (pieces of equipment) = 0.92
- Test-run 3: Drift = 0.03, 5.7 (pieces of equipment)/6 (pieces of equipment) = 0.95
- Test-run 4: Drift = 0.03, 5.7 (pieces of equipment)/6 (pieces of equipment) = 0.95

Volatility data represent the average value of each Test-run.

TABLE 3. Correspondence between the table labels and the Test-run number

	Table number	Production process	Working time	Volatility
Test-run 1	Table 4	Asynchronous process	627 (min)	0.29
Test-run 2	Table 6	Synchronous process	500 (min)	0.06
Test-run 3	Table 8	“Synchronization with preprocess” method	470 (min)	0.03
Test-run 4	Table 10	“Synchronization with preprocess” method	470 (min)	0.03

TABLE 4. Test-run 1

	WS	S1	S2	S3	S4	S5	S6
K1	15	20	20	25	20	20	20
K2	20	22	21	22	21	19	20
K3	10	20	26	25	22	22	26
K4	20	17	15	19	18	16	18
K5	15	15	20	18	16	15	15
K6	15	15	15	15	15	15	15
K7	15	20	20	30	20	21	20
K8	20	29	33	30	29	32	33
K9	15	14	14	15	14	14	14
Total	145	172	184	199	175	174	181

TABLE 5. Test-run 1 (Volatility of Table 4)

K1	1.67	1.67	3.33	1.67	1.67	1.67
K2	2.33	2	2.33	2	1.33	1.67
K3	1.67	3.67	3.33	2.33	2.33	3.67
K4	0.67	0	1.33	1	0.33	1
K5	0	1.67	1	0.33	0	0
K6	0	0	0	0	0	0
K7	1.67	1.67	5	1.67	2	1.67
K8	4.67	6	5	4.67	5.67	6
K9	0.33	0.33	0	0.33	0.33	0.33

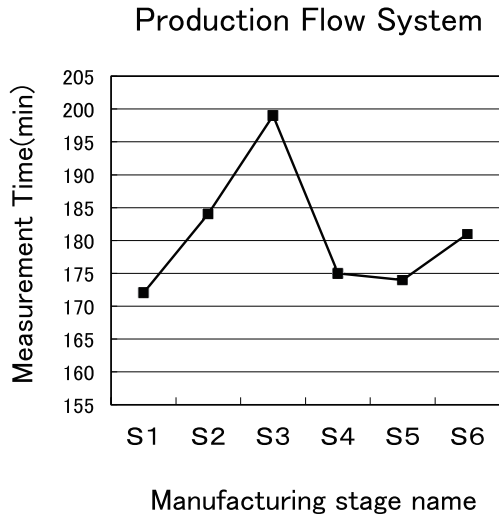


FIGURE 9. Total work time for each stage (S1-S6) in Table 4

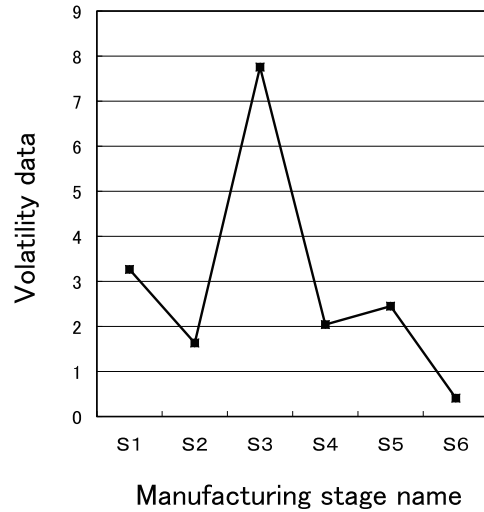


FIGURE 10. Volatility data for each stage (S1-S6) in Table 4

TABLE 6. Test-run2

	WS	S1	S2	S3	S4	S5	S6
K1	20	20	24	20	20	20	20
K2	20	20	20	20	20	22	20
K3	20	20	20	20	20	20	20
K4	20	25	25	20	20	20	20
K5	20	20	20	20	20	20	20
K6	20	20	20	20	20	20	20
K7	20	20	20	20	20	20	20
K8	20	27	27	22	23	20	20
K9	20	20	20	20	20	20	20
Total	180	192	196	182	183	182	180

TABLE 7. Test-run 2 (Volatility of Table 6)

K1	0	1.33	0	0	0	0
K2	0	0	0	0	0.67	0
K3	0	0	0	0	0	0
K4	1.67	1.67	0	0	0	0
K5	0	0	0	0	0	0
K6	0	0	0	0	0	0
K7	0	0	0	0	0	0
K8	2.33	2.33	0.67	1	0	0
K9	0	0	0	0	0	0

TABLE 8. Test-run 3

	WS	S1	S2	S3	S4	S5	S6
K1	20	18	19	18	20	20	20
K2	20	18	18	18	20	20	20
K3	20	21	21	21	20	20	20
K4	20	13	11	11	20	20	20
K5	20	16	16	17	20	20	20
K6	20	18	18	18	20	20	20
K7	20	14	14	13	20	20	20
K8	20	22	22	20	20	20	20
K9	20	25	25	25	20	20	20
Total	180	165	164	161	180	180	180

TABLE 9. Test-run 3 (Volatility of Table 8)

K1	0.67	0.33	0.67	0	0	0
K2	0.67	0.67	0.67	0	0	0
K3	0.33	0.33	0.33	0	0	0
K4	2.33	3	3	0	0	0
K5	1.3	1.3	1	0	0	0
K6	0.67	0.67	0.67	0	0	0
K7	2	2	2.3	0	0	0
K8	0.67	0.67	0	0	0	0
K9	1.67	1.67	1.67	0	0	0

